

Interaction-induced enhancement of the efficiency in a quantum Hall thermal machine

S. Finocchiaro,^{1,2} D. Ferraro,^{3,4} M. Sassetti,^{3,4} and G. Benenti^{1,2}

¹*Center for Nonlinear and Complex Systems, Dipartimento di Scienza e Alta Tecnologia, Università degli Studi dell'Insubria, Via Valleggio 11, 22100 Como, Italy*

²*Istituto Nazionale di Fisica Nucleare, Sezione di Milano, Via Celoria 16, 20133 Milano, Italy*

³*Dipartimento di Fisica, Università di Genova, Via Dodecaneso 33, 16146, Genova, Italy*

⁴*SPIN-CNR, Via Dodecaneso 33, 16146, Genova, Italy*

(Dated: November 26, 2024)

We investigate a thermal machine based on a single closed quantum Hall edge channel forming a quantum dot. It is tunneling coupled with two quantum Hall states at $\nu = 2$ kept at different temperatures, the hot one being also driven out-of-equilibrium by means of a periodic train of Lorentzian voltage pulses. This geometry is ideal to characterize the role played by the electron-electron interaction present within these channels on the efficiency of the machine. Here, it is possible to identify regions in the parameter space where the interaction leads to an improvement of the performances of the devices.

I. INTRODUCTION

Since the first industrial revolution, the possibility to efficiently convert heat into useful work played a central role in boosting the technological development of thermal machines. The study of the physical principles behind this transformation led to the emergence of thermodynamics^{1,2}.

Recent advances in miniaturization have triggered the interest into devices able to convert heat into work at the microscopic level, paving the way for the rapidly growing field of quantum thermodynamics^{3–16}. Indeed, the study of thermodynamics for microscopic and mesoscopic devices out-of-equilibrium actually requires a by far non-trivial extension of conventional thermodynamics towards the quantum realm. This is due to the fact that in nanodevices genuine non-classical effects play a crucial role and fundamental concepts such as heat and work need to be properly reconsidered.

A deep understanding of these basic concepts at the quantum level, represents therefore a fundamental starting point for designing highly performant quantum thermal machines^{17–20}. A first principles approach to the problem, starting from the non-classical properties that underlie the phenomenological laws of heat and particle transport, has proven particularly suitable for studying systems at the mesoscopic scale^{21–23}, demonstrating the potential to enhance the thermoelectric figure of merit in these systems. In this context, theoretical works have led to the possibility of controlling heat currents and designing thermal diodes, transistors, and thermal logic gates^{24,25}.

Among the main questions emerging in this field of research stands out the possibility to achieve high efficiency in miniaturized thermal machines operating out-of-equilibrium. As recently demonstrated theoretically, an ideal test-bed to address this problem is represented by a quantum dot tunneling coupled with two non-interacting chiral edge channels at filling factor $\nu = 1$.

They play the role of terminals kept at different temperatures and chemical potentials. In addition, the hot one is driven out-of-equilibrium by a periodic voltage. In this configuration, thanks also to the chirality of the edge states composing the reservoirs, such a system can reach a very high efficiency, and its performance is constrained by a non universal out-of-equilibrium bound which depends on the applied drive²⁶. The latter is derived directly imposing the positivity on the entropy production¹¹.

An interesting, but still largely unexplored, aspect in this direction is the proper characterization of the role played by interaction and quantum correlations in modifying the efficiency of thermoelectric machines²⁷. Remarkably enough, quantum Hall edge states are the ideal playground to study interaction effects in low dimension^{28,29}. Indeed, here electron-electron interaction within and among the channels at the boundary of the quantum Hall bar can be treated exactly in terms of the so called chiral Luttinger liquid formalism^{30,31}.

In this work, we will address the role played by interactions in a quantum Hall thermal machine analogous to the one discussed in Ref. 26. However, here the terminals will be edge states at filling factor $\nu = 2$, namely composed by two co-propagating and interacting edge channels. The hot one will be further driven out-of-equilibrium by a properly quantized train of Lorentzian voltage pulses, usually called Levitons^{32,33}. Due to the electron-electron interaction such pulses shows spin-charge separation³⁴. We will demonstrate the emergence of regimes of parameter where the interaction leads to an enhancement of the efficiency.

The present paper is organized as follows. In Section II we will introduce the quantum thermal machine, discussing all the elements needed to properly characterize its functioning such as the edge-magnetoplasmon description of the quantum Hall edge channels and the photo-assisted tunneling through the quantum dot. Section III will describe the relevant physical quantities needed to

characterize the efficiency of the thermal machine under investigation, namely the charge and the heat currents flowing across the system as well as the power. In Section IV we will demonstrate the robustness of the efficiency with respect electron-electron interaction and its enhancement in a proper range of parameters. Section V will be devoted to the conclusions. Finally two Appendices will report some technical details of the calculations.

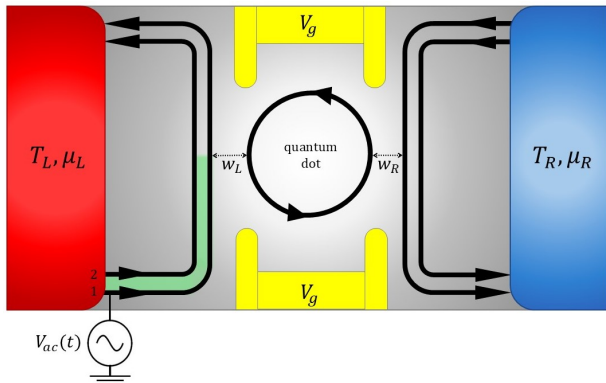


Figure 1: Scheme of a quantum Hall thermal machine. The terminals are quantum Hall states at filling factor $\nu = 2$ kept at a given chemical potentials μ_R, μ_L and temperatures T_R, T_L respectively by means of two reservoirs (red and blue). The choice of colors has been done to visually show that $T_L > T_R$, characterizing the left as the hot terminal. It is also driven out of equilibrium by applying an ac drive $V_{ac}(t)$ to its outer channel. Thanks to the action of gate voltages V_g the two terminals are tunneling coupled with amplitudes w_R and w_L respectively to a Hall quantum dot at filling factor $\nu = 1$. The numbers 1 and 2 denote the outer and inner channels respectively, and the green area represents the interaction region.

II. MODEL

A. Description of the set-up

We consider a quantum thermal machine based on a Hall quantum dot, namely a system with a discrete energy spectrum realized by a closed quantum Hall edge state, tunneling coupled with external right (R) and left (L) chiral edge states playing the role of terminals. They are kept at different chemical potentials μ_R and μ_L , and temperatures T_R and T_L respectively. In the following, we will assume L as the hot terminal, namely $T_L > T_R$. Moreover, it is also driven out-of-equilibrium by an additional periodic ac voltage applied to its outer channel (see Fig. 1). We assume here that the gate voltages (V_g) are chosen in such a way that the quantum dot is composed by a unique closed channel (at filling factor $\nu = 1$), while the terminals are at filling factor $\nu = 2$, namely

they are composed by two co-propagating edge channels. In this configuration the electron-electron interaction among the edge states in the terminals need to be taken into account. In the following, we will analyze step by step all the relevant parts of this thermal machine in order to properly characterize its performance in the present case.

B. Interacting quantum Hall edge channels at $\nu = 2$

As usually done in the literature on the subject, we assume that each one of the two edge states at filling factor $\nu = 2$, forming the terminals, is composed by channels interacting within a region of finite length \mathcal{L} via a screened Coulomb repulsion^{34–42}. This modelization has been crucial to explain various experimental observations^{43–46}. To properly describe the system under this condition we need to consider the so called chiral Luttinger liquid picture³⁰, where the edge states are described in terms of bosonic modes chirally propagating along the edge, usually dubbed edge-magnetoplasmons^{37,38,47}. Within this picture the Hamiltonian density of each edge in the interacting region can be written as

$$\mathcal{H} = \sum_{\alpha=1,2} \frac{\hbar v_i}{4\pi} (\partial_x \phi_\alpha(x))^2 + \frac{\hbar u}{2\pi} (\partial_x \phi_1(x)) (\partial_x \phi_2(x)), \quad (1)$$

where the index $\alpha = 1, 2$ labels the outer and inner channel respectively (see Fig. 2), while ϕ_α are chiral bosonic fields satisfying the commutation relations

$$[\phi_\alpha(x), \phi_\beta(y)] = i\pi \text{sign}(x-y) \delta_{\alpha,\beta}. \quad (2)$$

They are related to the particle density operator by

$$\rho_\alpha(x) = \frac{1}{2\pi} \partial_x \phi_\alpha(x). \quad (3)$$

The annihilation operator for an electron in the channel $\alpha = 1, 2$ can be written as a coherent state of the bosonic fields introduced above in such a way that

$$\psi_\alpha(x) = \frac{\mathcal{F}_\alpha}{\sqrt{2\pi a}} e^{-i\phi_\alpha(x)} \quad (4)$$

with a a short distance cut-off and \mathcal{F}_α playing the role of Klein factors^{30,31,48}. In Eq. (1) $v_1 \geq v_2$ are the bare propagation velocities of the two edge channels and u is the intensity of the density-density coupling among the edges.

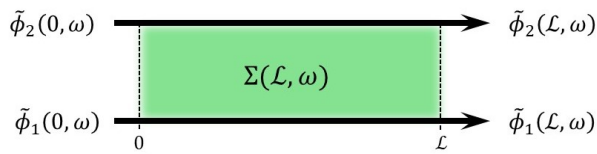


Figure 2: Scheme of a quantum Hall edge state at filling factor $\nu = 2$. The interaction region of finite length \mathcal{L} between the two channels is indicated by the green area. In the frequency domain the incoming bosonic fields and the outgoing ones are denoted by $\tilde{\phi}_{1/2}(0, \omega)$ and $\tilde{\phi}_{1/2}(\mathcal{L}, \omega)$ respectively and are connected by the edge-magnetoplasmon scattering matrix $\Sigma(\mathcal{L}, \omega)$.

The Hamiltonian in Eq. (1) can be diagonalized through the rotation in the bosonic space⁴¹ of angle

$$\theta = \frac{1}{2} \arctan\left(\frac{2u}{v_1 - v_2}\right). \quad (5)$$

This parameter encodes the interaction strength, indeed $\theta = 0$ corresponds to the non-interacting case while $\theta = \pi/4$ represents the strong interacting limit^{36,49,50}. The rotation leads to a charged and dipolar bosonic fields defined respectively as

$$\phi_\rho(x) = \phi_1(x) \cos \theta + \phi_2(x) \sin \theta \quad (6)$$

$$\phi_\sigma(x) = -\phi_1(x) \sin \theta + \phi_2(x) \cos \theta \quad (7)$$

with the full diagonalized Hamiltonian density assuming the form

$$\mathcal{H} = \frac{\hbar v_\rho}{4\pi} (\partial_x \phi_\rho(x))^2 + \frac{\hbar v_\sigma}{4\pi} (\partial_x \phi_\sigma(x))^2 \quad (8)$$

with

$$v_{\rho/\sigma} = \left(\frac{v_1 + v_2}{2}\right) \pm \frac{1}{\cos(2\theta)} \left(\frac{v_1 - v_2}{2}\right). \quad (9)$$

As schematically illustrated in Fig. 2, moving to the Fourier space (indicated in the following with the upper tilde notation) the dynamics of the edge channels can be solved within a scattering matrix formalism³⁷, namely the component at frequency ω of the fields outgoing from an interacting region at finite length \mathcal{L} is related to incoming ones by

$$\begin{pmatrix} \tilde{\phi}_1(\mathcal{L}, \omega) \\ \tilde{\phi}_2(\mathcal{L}, \omega) \end{pmatrix} = \Sigma(\mathcal{L}, \omega) \begin{pmatrix} \tilde{\phi}_1(0, \omega) \\ \tilde{\phi}_2(0, \omega) \end{pmatrix} \quad (10)$$

with

$$\Sigma = \begin{pmatrix} \cos^2 \theta e^{i\omega\tau_\rho} + \sin^2 \theta e^{i\omega\tau_\sigma} & \sin \theta \cos \theta (e^{i\omega\tau_\rho} - e^{i\omega\tau_\sigma}) \\ \sin \theta \cos \theta (e^{i\omega\tau_\rho} - e^{i\omega\tau_\sigma}) & \sin^2 \theta e^{i\omega\tau_\rho} + \cos^2 \theta e^{i\omega\tau_\sigma} \end{pmatrix}. \quad (11)$$

Notice that, in the above expression we have introduced the times of flight $\tau_{\rho/\sigma} = \mathcal{L}/v_{\rho/\sigma}$.

We can now consider an ohmic contact applying a purely ac voltage $V_{ac}(t)$ only to the outer channels of

the L terminal (see Fig. 1). This can be model by means of the additional contribution to the density Hamiltonian

$$\mathcal{H}_U = -e \int \rho_1(x) U(x, t) dx, \quad (12)$$

where $U(x, t) = \Theta(-x)V_{ac}(t)$ with $\Theta(-x)$ the Heaviside step function and $-e$ the electron charge^{51,52}.

This classical voltage creates a coherent state for the edge-magnetoplasmons along the edge channels^{34,53}. In the frequency domain the interacting region acts as a beam-splitter for this coherent state through the edge-magnetoplasmon scattering matrix $\Sigma(\mathcal{L}, \omega)$ in exactly the same way as for the bosonic modes in absence of voltage. According to this, the voltages outgoing from the interacting region can be written as

$$\begin{pmatrix} \tilde{V}_{1,out}(\omega) \\ \tilde{V}_{2,out}(\omega) \end{pmatrix} = \Sigma(\mathcal{L}, \omega) \begin{pmatrix} \tilde{V}_{ac}(\omega) \\ 0 \end{pmatrix}. \quad (13)$$

Going back to the time domain this leads to

$$\begin{aligned} V_{1,out}(t) &= \cos^2 \theta V_{ac}(t - \tau_\rho) + \sin^2 \theta V_{ac}(t - \tau_\sigma) \\ V_{2,out}(t) &= \sin \theta \cos \theta [V_{ac}(t - \tau_\rho) - V_{ac}(t - \tau_\sigma)] \end{aligned} \quad (14)$$

which is a manifestation of the so called spin-charge separation of the applied voltage^{34,39}. It is worth to note that, according to Eq. (14), a time-independent voltage is not affected by the presence of interaction.

Taking into account the above analysis, in the following we will consider the tunneling of electrons from the outgoing channels of the reservoirs to the quantum dot in presence of the modified voltage $V_{1,out}(t)$. This tunneling will be assumed to occur in absence of interaction due to the presence of additional screening of the Coulomb interaction at the level of the quantum point contacts illustrated in Fig. 1. Before doing this, however, it is useful to characterize the tunneling across the central quantum dot in absence of the applied time dependent voltage.

C. Tunneling through the quantum dot

As stated above, we consider a quantum dot made only by one closed channel ($\nu = 1$). In this configuration, we also choose the geometry of the dot and consequently its level spacing in such a way that only one energy level, with given energy E_0 , is relevant for our analysis. More specifically, due to the fact that the level spacing of the quantum dot scales as the inverse of its circumference, this situation is achieved for a small enough quantum dot.

Considering a local electron tunneling occurring only at the level of the outer edge channels of the terminals in absence of interaction it is possible to introduce a new (fermionic) 2×2 scattering matrix \mathbb{S} connecting the electrons incoming into the dot to the outgoing ones. It is unitary ($\mathbb{S}^\dagger \mathbb{S} = \mathbb{I}_{2 \times 2}$) and assumes the general form

$$\mathbb{S}(E) = \begin{pmatrix} S_{LL}(E) & S_{LR}(E) \\ S_{RL}(E) & S_{RR}(E) \end{pmatrix}, \quad (15)$$

where the notation $S_{jk}(E)$, with $j, k \in L, R$, keeps track of the part of the set-up from where the electron enters the dot (k) and to where it goes out (j). Due to the overall constraints of the scattering matrix one has

$$|S_{RL}(E)|^2 = |S_{LR}(E)|^2. \quad (16)$$

In order to proceed further with respect to these general statements, it is possible to write down an explicit for the scattering matrix of the quantum dot^{54,55}. Taking into account the fact that the dot has a unique relevant energy level and considering the tunneling amplitudes w_j ($j = L, R$) for an electron to jump from the j -th terminal to the dot one can write

$$\mathbb{S}(E) = \mathbb{I}_{2 \times 2} - \frac{2i\pi}{E - E_0 + i\pi(|w_L|^2 + |w_R|^2)} \begin{pmatrix} |w_L|^2 & w_L^* w_R \\ w_R^* w_L & |w_R|^2 \end{pmatrix}, \quad (17)$$

which satisfies the general properties discussed above. In particular, one has

$$|S_{RL}(E)|^2 = |S_{LR}(E)|^2 = \frac{\Gamma_L \Gamma_R}{(E - E_0)^2 + \frac{1}{4}(\Gamma_L + \Gamma_R)^2} \quad (18)$$

where we have introduced the short notation $\Gamma_j = 2\pi|w_j|^2$. Here, Γ_j/\hbar are the decay rates of the state of the dot associated to the emission of an electron into the j -th terminal. From the above expression, we notice that the transmission associated to the dot is a Breit-Wigner function peaked at $E = E_0$ and with width given by $\Gamma_L + \Gamma_R$. In the following, for sake of simplicity, we will assume a symmetric set-up with $\Gamma_L = \Gamma_R = \Gamma/2$, with Γ considered as the unit for the energies, and we will consider $E_0 = 0$ as the reference of the energies.

1. Photo-assisted electron tunneling

We want now to extend the previous discussion to include the effects of the periodic drive $V_{ac}(t)$ applied to the outer channel of the hot terminal L . It is worth to note that, in spite of the changes of the overall profile of the voltage due to interaction effects encoded in Eq. (14), the periodicity of the drive affecting the electron before the tunneling is preserved, namely $V_{1,out}(t) = V_{1,out}(t + \mathcal{T})$ with \mathcal{T} the period of the applied drive. This leads to the Fourier series

$$e^{-i\frac{e}{\hbar} \int_0^t V_{1,out}(t') dt'} = \sum_{l=-\infty}^{+\infty} \mathcal{P}_l(q) e^{-il\Omega t} \quad (19)$$

where $\Omega = 2\pi/\mathcal{T}$ and

$$q = \frac{-eV_0}{\hbar\Omega} \quad (20)$$

with V_0 the amplitude of the incoming ac drive (see below for more details). In the above expression the coefficients

\mathcal{P}_l are the probability amplitude for an electron to absorb (emit) l photons for $l > 0$ ($l < 0$) due to the drive³³. They can be written as⁴¹

$$\mathcal{P}_l(q) = \sum_{n=-\infty}^{+\infty} p_{l-n}(q \cos^2 \theta) p_n(q \sin^2 \theta) \times e^{i\Omega\tau_\rho(l-n)} e^{i\Omega\tau_\sigma(n)}, \quad (21)$$

where the coefficients p_l are defined as

$$p_l(q) = \frac{\Omega}{2\pi} \int_0^{\frac{2\pi}{\Omega}} dt e^{-i\frac{e}{\hbar} \int_0^t dt' V_{ac}(t')} e^{il\Omega t}. \quad (22)$$

Within this photo-assisted tunneling picture it is possible to extend the previous analysis by introducing the so called Floquet scattering matrix for the dot in presence of a driven lead given by⁵⁶⁻⁵⁸

$$\mathbb{S}^{(F)}(E_n, E) = \begin{pmatrix} S_{LL}^{(F)}(E_n, E) & S_{LR}^{(F)}(E_n, E) \\ S_{RL}^{(F)}(E_n, E) & S_{RR}^{(F)}(E_n, E) \end{pmatrix} = \begin{pmatrix} \mathcal{P}_n(q) S_{LL}(E_n) & \delta_{n,0} S_{LR}(E) \\ \mathcal{P}_n(q) S_{RL}(E_n) & \delta_{n,0} S_{RR}(E) \end{pmatrix}, \quad (23)$$

with $E_n = E + n\hbar\Omega$. Notice that in the above expression the effect of interaction is encoded in the $\mathcal{P}_n(q)$.

In the following, we will report the expressions for the relevant physical quantities needed to characterize the efficiency of such thermal machine charge within this formalism.

III. RELEVANT PHYSICAL QUANTITIES

A. Currents

Defining the photo-assisted transmission amplitudes

$$\tau_{RL}(E) \equiv \sum_n |S_{RL}^{(F)}(E_n, E)|^2 \quad (24)$$

$$\tau_{LR}(E) \equiv \sum_n |S_{LR}^{(F)}(E_n, E)|^2, \quad (25)$$

the average number of photons absorbed or emitted during the scattering process

$$\langle n(E) \rangle_{jk} = \sum_n n |S_{jk}^{(F)}(E_n, E)|^2 \quad (26)$$

and the Fermi distribution of the reservoirs in absence of time-dependent drive

$$f_{R/L}(E) = \frac{1}{1 + e^{\frac{E - \mu_{R/L}}{k_B T_j}}} \quad (27)$$

it is possible to write down compact expressions for the average currents flowing across the system in one period \mathcal{T} . In particular, the charge currents are given by⁵⁶

$$I_R^e = -\frac{e}{h} \int_{-\infty}^{+\infty} dE [\tau_{RL}(E)f_L(E) - \tau_{LR}(E)f_R(E)], \quad (28)$$

$$I_L^e = -\frac{e}{h} \int_{-\infty}^{+\infty} dE [\tau_{LR}(E)f_R(E) - \tau_{RL}(E)f_L(E)], \quad (29)$$

naturally satisfying $I_R^e = -I_L^e$ due to charge conservation. Analogously the heat currents are given by^{57,59}

$$I_R^h = \int_{-\infty}^{+\infty} \frac{dE}{h} (E - \mu_R) [\tau_{RL}(E)f_L(E) - \tau_{LR}(E)f_R(E)] + \frac{\Omega}{2\pi} \sum_{k=L,R} \int_{-\infty}^{+\infty} dE \langle n(E) \rangle_{Rk} f_k(E), \quad (30)$$

$$I_L^h = \int_{-\infty}^{+\infty} \frac{dE}{h} (E - \mu_L) [\tau_{LR}(E)f_R(E) - \tau_{RL}(E)f_L(E)] + \frac{\Omega}{2\pi} \sum_{k=L,R} \int_{-\infty}^{+\infty} dE \langle n(E) \rangle_{Lk} f_k(E). \quad (31)$$

B. Power and efficiency

The power generated by the system within one period is given in general by the difference of two contributions

$$P_{gen} = P_e - P_{in}. \quad (32)$$

The first term corresponds to the electric power produced by the system due to the difference in the chemical potentials and is given by

$$P_e = -\Delta V I_R^e \quad (33)$$

with $\Delta V = (\mu_R - \mu_L)/e$. This quantity will be chosen in such a way to maximize the electric power P_e according to the procedure discussed in detail in Appendix A.

The second term in Eq. (32) is related to the energy injected by the applied periodic drive and reads (see Appendix B for more details on the derivation)

$$\begin{aligned} P_{in} &= -\Delta V I_R^e + I_L^h + I_R^h \\ &= \frac{\Omega}{2\pi} \sum_{jk} \int_{-\infty}^{+\infty} dE \langle n(E) \rangle_{jk} f_k(E), \end{aligned} \quad (34)$$

which depend on the change of the electron energy associated to the absorption and emission of photons. An interesting feature of the considered system is the fact that, in the case of ideal chiral channels, $P_{in} = 0$ independently of the form of the applied ac drive²⁶. This can be demonstrated as follows. We can expand Eq. (34) in such a way that

$$P_{in} = \frac{\Omega}{2\pi} \int_{-\infty}^{+\infty} dE f_L(E) [\langle n(E) \rangle_{LL} + \langle n(E) \rangle_{RL}], \quad (35)$$

where we have taken into account the fact that

$$\langle n(E) \rangle_{RR} = \langle n(E) \rangle_{LR} = 0, \quad (36)$$

because the electrons coming from the terminal R are not affected by a periodic drive. Moreover, one has

$$\sum_{j=R,L} \langle n(E) \rangle_{jL} = \sum_n n |\mathcal{P}_n|^2 = \frac{e}{h} \int_0^{\frac{2\pi}{\Omega}} dt V_{1,out}(t) = 0. \quad (37)$$

This finally leads to the relation

$$P_{gen} = P_e. \quad (38)$$

Two remarks are in order at this point. First of all this result is a consequence of the Landauer-Büttiker picture for ideal one dimensional ballistic edge channels⁶⁰. It is expected that more realistic situations would lead to non-zero values of P_{in} ⁶¹. Moreover, it is worth to mention that the above arguments do not apply to the case of non-chiral edge channels, where P_{in} is in general different from zero²⁶.

Thank to the above considerations, it is now possible to define the efficiency of the considered thermal machine as

$$\eta = \frac{P_{gen}}{-I_L^h} \quad (39)$$

in such a way that one has $\eta > 0$ for a thermal engine with $P_{gen} > 0$ absorbing heat from the L reservoir. It is worth to note that the above definition of the efficiency depends on the interaction θ between the channel composing the terminal L .

IV. RESULTS

We have now all the ingredients needed to investigate the efficiency of the present thermal machine as a function of the interaction between the edge channels composing the terminals. To be more precise, according to the previous discussions, what really matter is the presence of interaction in the terminal L driven out-of-equilibrium. To fix the ideas, in the following we will consider as applied periodic drive $V_{ac}(t)$ a train of Lorentzian pulses, of width \mathcal{W} and period \mathcal{T} , of the form

$$V_{ac}(t) = V_0 \left[\frac{1}{\pi} \sum_{k=-\infty}^{+\infty} \frac{\delta}{\delta^2 + \left(\frac{t}{\mathcal{T}} - k\right)^2} - 1 \right], \quad (40)$$

where $\delta = \mathcal{W}/\mathcal{T}$ and such that $-eV_0 = q\hbar\Omega$, with q a parameter that will be specified in the following. Note that this potential has zero average over one period as expected for a purely ac drive.

As theoretically predicted by Levitov and coworkers^{32,62,63} and experimentally demonstrated by D. C. Glattli and his group⁶⁴⁻⁶⁷ this kind of drive, by imposing the quantization condition $q \in \mathbb{N}$, leads to the injection of purely electronic excitations, usually dubbed Levitons, without introducing in the system any electron-hole pair. In the following, for sake of simplicity, we will set $q = 1$.

Moreover the width of the pulses and the period will be chosen within an experimentally achievable range⁶⁸.

For a periodic potential of the form in Eq. (40) the coefficients $p_l(q)$ are given by^{33,34,51,69}

$$p_l(q) = q \sum_{s=0}^{+\infty} \frac{(-1)^s \Gamma(q+l+s) e^{-2\pi\delta(2s+l)}}{\Gamma(q+1-s)\Gamma(1+s)\Gamma(1+l+s)}, \quad (41)$$

with $\Gamma(\dots)$ the Euler's Gamma function. Thus, the photo-assisted amplitudes $\mathcal{P}_l(q)$ are completely specified by Eq. (21) (fixing $q = 1$ as stated above).

Applying the formalism described above, we can now calculate the efficiency η of the thermal machine under investigation as a function of the average chemical potential $\mu = (\mu_L + \mu_R)/2$ and the driving frequency Ω for different values of the interaction strength.

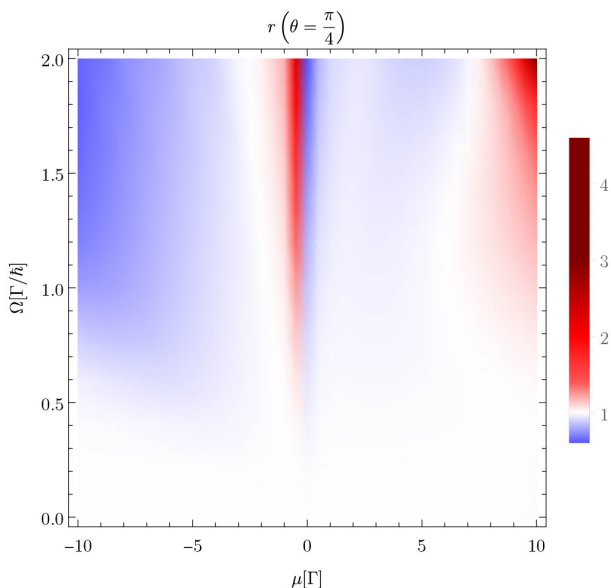


Figure 3: Density plot of the ratio $r(\theta) = \eta(\theta)/\eta(0)$ as a function of μ (in units of Γ) and Ω (in units of Γ/\hbar). The considered parameters are: $T_L = 0.061 K$, $T_R = 0.055 K$, $\tau_\rho = 7.5 \times 10^{-12} s$, $\tau_\sigma = 1.5 \times 10^{-11}$, $q = 1$, $\delta = 0.05$, $\Gamma = 0.02$ meV and $\theta = \pi/4$.

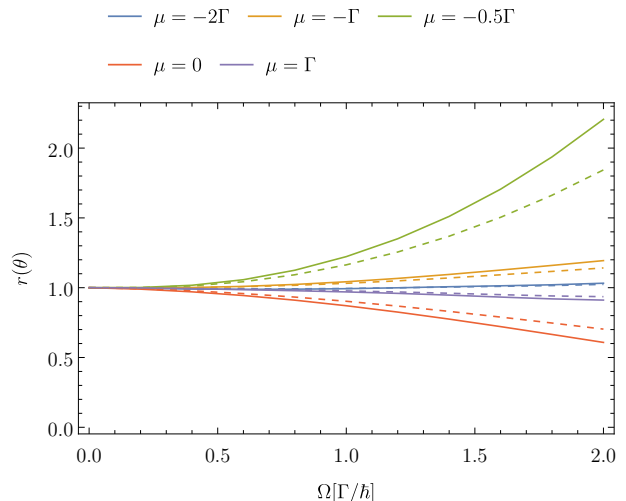


Figure 4: Plots of $r(\theta)$ as functions of Ω (in units of Γ/\hbar), evaluated for $\mu = -2\Gamma$ (blue curves), $\mu = -\Gamma$ (yellow curves), $\mu = -0.5\Gamma$ (green curves), $\mu = 0$ (orange curves) and $\mu = \Gamma$ (violet curves). For each value of μ the interaction strength is set at $\theta = \pi/4$ (solid line) and $\theta = \pi/6$ (dashed line). The other considered parameters are: $T_L = 0.061 K$, $T_R = 0.055 K$, $\tau_\rho = 7.5 \times 10^{-12} s$, $\tau_\sigma = 1.5 \times 10^{-11}$, $q = 1$, $\delta = 0.05$ and $\Gamma = 0.02$ meV.

In the density plot in Fig. 3 we show the ratio

$$r(\theta) = \frac{\eta(\theta)}{\eta(0)} \quad (42)$$

between the efficiency in presence of interaction and the one evaluated for the free electron case. Both these quantities are obtained in correspondence of the maximum power achieved according to the procedure reported in Appendix A. From this plot we can deduce that, focusing on the maximum achievable value of the interaction $\theta = \pi/4$, there are regions of the parameters space where the interaction leads to an enhancement of the efficiency (red zones in the density plot). Actually, for the majority of the values considered for the parameters, the interaction slightly reduces the efficiency. However, an enhancement of efficiency due to interactions is observed for $\mu < 0$, in an interval approximately around $-1.5\Gamma \lesssim \mu \lesssim 0$, and for $\mu \approx 10$. Both these regions widen as the frequency increases. In addition, we note that the effects of the interaction becomes progressively more evident by rising the frequency, namely approaching timescales of the order of the typical separation between the charged and the dipolar modes ($\Omega^{-1} \approx \tau_\sigma - \tau_\rho$).

By lowering the intensity of the interaction the observed enhancement decreases (see green and orange curves of Fig. 4) but still present as a signature of the relative robustness of the observed effect. Moreover, the observed enhancement is progressively more evident, at high enough frequency and at fixed average temperature T , by lowering the temperature difference ΔT between the two terminal. This is shown in Fig.5.

From the above considerations one can deduce that, within a convenient range of parameters, it is possible to exploit the interaction between the two edge channels of the hot terminal in order to improve the efficiency of the thermal machine with respect to the non-interacting case.

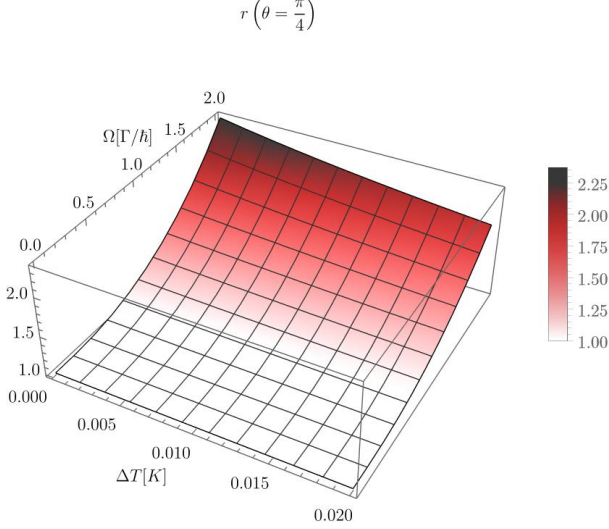


Figure 5: 3D plot of the ratio $r(\theta)$ as a function of ΔT and Ω (in units of Γ/\hbar), at fixed average potential $\mu = -0.5\Gamma$. The considered parameters are: $T = 0.058 K$, $\tau_\rho = 7.5 \times 10^{-12} s$, $\tau_\sigma = 1.5 \times 10^{-11}$, $q = 1$, $\delta = 0.05$, $\Gamma = 0.02$ meV and $\theta = \pi/4$.

V. CONCLUSIONS

We have studied a quantum thermal machine based on a small closed Hall channel at filling factor $\nu = 1$, tunneling coupled to two terminals realized by quantum Hall states at $\nu = 2$ and placed at different temperatures and chemical potentials. The hot terminal is also driven out-of-equilibrium by means of the application of a periodic train of Lorentzian voltage pulses. Due to the presence of electron-electron interaction between the two edge channels composing the terminal such pulses fractionalize. Under these conditions we have been able to treat exactly the problem identifying regions in the parameter space, notably high frequencies of the applied drive and small temperature differences between the terminals, where the interaction leads to an improvement the performances of the devices. This analysis will open new perspectives in the realization of more performant quantum thermal machines exploiting interaction and correlation to enhance the efficiency.

Future developments in this work could address systems based on helical edge states of a two-dimensional topological insulator⁷⁰⁻⁷², fractional quantum Hall edge channels^{30,73-75} and more involved topological systems⁷⁷.

Acknowledgments

Authors would like to thank R. Lopez, T. Martin, M. Moskalets, F. Ronetti and S. Ryu for useful discussions. D.F. acknowledges the contribution of the European Union-NextGenerationEU through the ‘‘Quantum Buses for Coherent Energy Transfer’’ (QUBERT) project, in the framework of the Curiosity Driven 2021 initiative of the University of Genova. G.B. and D.F. acknowledge support from the project PRIN 2022 - 2022XK5CPX (PE3) SoS-QuBa - ‘‘Solid State Quantum Batteries: Characterization and Optimization’’ funded within the programme ‘‘PNRR Missione 4 - Componente 2 - Investimento 1.1 Fondo per il Programma Nazionale di Ricerca e Progetti di Rilevante Interesse Nazionale (PRIN)’’, funded by the European Union - Next Generation EU. G.B. acknowledge support from the Julian Schwinger Foundation (Grant JSF-21-04-0001) and from INFN through the project ‘‘QUANTUM’’.

Appendix A: Considerations about the choice of the potential difference ΔV

The voltage difference ΔV that maximize the electric power P_e can be evaluated in the framework of the linear response theory considering the first order expansion of the current I_R^e in ΔV and in the temperature difference ΔT . This is given by¹¹

$$I_R^e = I_0^e + G\Delta V + G\mathcal{S}\Delta T, \quad (\text{A1})$$

with G the electric conductance, \mathcal{S} the Seebeck coefficient, and I_0^e defined as

$$I_0^e = I_R^e|_{\Delta V=\Delta T=0} = \frac{-e}{h} \int_{-\infty}^{+\infty} dE [\tau_{RL}(E) - \tau_{LR}(E)] f(E), \quad (\text{A2})$$

where

$$f(E) = \frac{1}{e^{\frac{E-\mu}{k_B T}} + 1} \quad (\text{A3})$$

is the Fermi distribution evaluated at the average temperature $T = \frac{T_L + T_R}{2}$ and the average chemical potential $\mu = \frac{\mu_L + \mu_R}{2}$. The electric power output can then be written as

$$P_e = -\Delta V I_R^e = -\Delta V (I_0^e + G\Delta V + G\mathcal{S}\Delta T), \quad (\text{A4})$$

and reaches its maximum for

$$\Delta V = -\frac{1}{2}\mathcal{S}\Delta T - \frac{I_0^e}{2G}. \quad (\text{A5})$$

It is useful now to express the transport coefficients G and \mathcal{S} in terms of Onsager coefficients in such a way that¹¹

$$\mathcal{S} = \frac{1}{T} \frac{L_{eh}}{L_{ee}} \quad \text{and} \quad G = \frac{L_{ee}}{T}. \quad (\text{A6})$$

These quantities can be evaluated expanding the Fermi distributions $f_L(E)$ and $f_R(E)$ at first order around T and μ , and inserting them in the expressions of the currents. This leads to the following expressions:

$$L_{ee} = e^2 T \mathcal{I}^{(0)}, \quad (\text{A7})$$

$$L_{eh} = L_{he} = e T \mathcal{I}^{(1)}, \quad (\text{A8})$$

$$L_{hh} = T \mathcal{I}^{(2)}, \quad (\text{A9})$$

with

$$\mathcal{I}^{(n)} = \int_{-\infty}^{+\infty} \frac{dE}{h} (E - \mu)^n (-f'(E)) \frac{\tau_{RL}(E) + \tau_{LR}(E)}{2}. \quad (\text{A10})$$

According to this, the potential difference which maximizes the electric power is finally given by

$$\Delta V = -\frac{1}{2} \frac{\Delta T}{T} \frac{\mathcal{I}^{(1)}}{e \mathcal{I}^{(0)}}. \quad (\text{A11})$$

In Fig. 6 we report the density plot of ΔV , as a function of μ and Ω , evaluated for $\theta = 0$ (qualitatively similar results are obtained also in presence of interaction) for the ac voltage drive in Eq. (40). It is worth noting that, depending on the value of μ , this quantity assumes both positive (approximately for $\mu < 0$) and negative (approximately for $\mu > 0$) values.

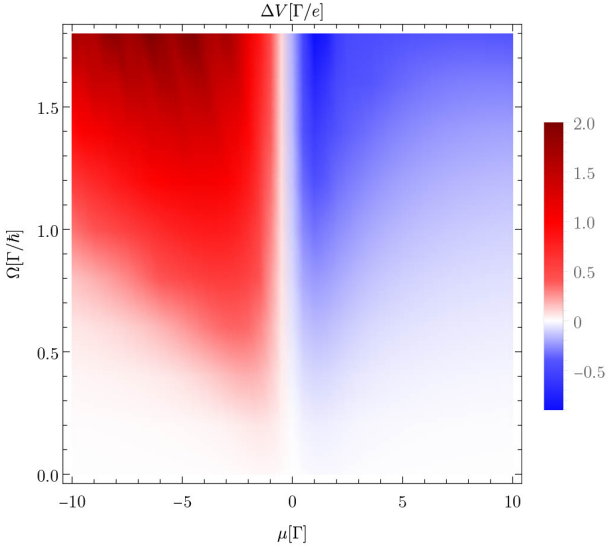


Figure 6: Density plot of ΔV , in units of Γ/e , as a function of μ (in units of Γ) and Ω (in units of Γ/\hbar). The interaction strength is $\theta = 0$. Other parameters are: $T_L = 0.061 K$, $T_R = 0.055 K$, $\delta = 0.05$, $q = 1$ and $\Gamma = 0.02 \text{ meV}$.

Appendix B: Derivation of Eq. (34)

The power injected in the system by the applied periodic drive can be expressed, directly using energy conservation during one period \mathcal{T} , as⁷⁶

$$P_{in} = I_L^u + I_R^u, \quad (\text{B1})$$

where $I_{R,L}^u$ are the energy currents flowing through the terminals. These currents can be written as

$$I_\alpha^u = \int_{-\infty}^{+\infty} \frac{dE}{h} E [f_\alpha^{out}(E) - f_\alpha(E)], \quad (\text{B2})$$

where $\alpha = L, R$ and f_α^{out} is defined as

$$f_\alpha^{out}(E) = \sum_{n=-\infty}^{+\infty} \sum_{\beta=L,R} |S_{\alpha\beta}^{(F)}(E, E_n)|^2 f_\beta(E_n). \quad (\text{B3})$$

The Fermi distribution $f_\alpha(E)$ can be rewritten as

$$f_\alpha(E) = \sum_{n=-\infty}^{+\infty} \sum_{\beta=L,R} \delta_{n0} \delta_{\alpha\beta} f_\beta(E_n), \quad (\text{B4})$$

in such a way that Eq. (B2) becomes

$$I_\alpha^u = \int_{-\infty}^{+\infty} \frac{dE}{h} \sum_{n=-\infty}^{+\infty} \sum_{\beta=L,R} [-\delta_{\alpha\beta} \delta_{n0} + |S_{\alpha\beta}^{(F)}(E, E_n)|^2] E f_\beta(E_n). \quad (\text{B5})$$

Making the substitution $E \rightarrow E - n\hbar\Omega$ in the integral and replacing n with $-n$, one obtains

$$I_\alpha^u = \int_{-\infty}^{+\infty} \frac{dE}{h} \sum_{n=-\infty}^{+\infty} \sum_{\beta=L,R} [-\delta_{\alpha\beta} \delta_{n0} + |S_{\alpha\beta}^{(F)}(E_n, E)|^2] E_n f_\beta(E). \quad (\text{B6})$$

It is now possible to write explicit expressions of the two energy currents. Focusing for example on $\alpha = R$, Eq. (B6) reads

$$I_R^u = \int_{-\infty}^{+\infty} \frac{dE}{h} \sum_n \{ [-\delta_{n0} + |S_{RR}^{(F)}(E_n, E)|^2] E_n f_R(E) + |S_{RL}^{(F)}(E_n, E)|^2 E_n f_L(E) \}. \quad (\text{B7})$$

Recalling that $E_n = E + n\hbar\Omega$ and using the unitarity of the scattering matrix, one has

$$\begin{aligned} I_R^u &= \int_{-\infty}^{+\infty} \frac{dE}{h} \sum_n \{ [-\delta_{n0} + |S_{RR}^{(F)}(E_n, E)|^2] (E + n\hbar\Omega) f_R(E) + \\ &+ |S_{RL}^{(F)}(E_n, E)|^2 (E + n\hbar\Omega) f_L(E) \} = \\ &= \int_{-\infty}^{+\infty} \frac{dE}{h} \left\{ \left(-\sum_n |S_{LR}^{(F)}(E_n, E)|^2 \right) E f_R(E) + \right. \\ &+ \sum_n |S_{RL}^{(F)}(E_n, E)|^2 E f_L(E) + \\ &\left. + \hbar\Omega \sum_n n [|S_{RR}^{(F)}(E_n, E)|^2 f_R(E) + |S_{RL}^{(F)}(E_n, E)|^2 f_L(E)] \right\}. \end{aligned} \quad (\text{B8})$$

Considering the definitions given in Eqs. (24), (25), and (26), it is useful to write the energy current in terms of photo-assisted transmission amplitudes and average number of the photon exchanged in the scattering process

as

$$I_R^u = \int_{-\infty}^{+\infty} \frac{dE}{h} E [\tau_{RL}(E) f_L(E) - \tau_{LR}(E) f_R(E)] + \frac{\Omega}{2\pi} \sum_{\beta=L,R} \int_{-\infty}^{+\infty} dE \langle n(E) \rangle_{R\beta} f_\beta(E). \quad (\text{B9})$$

Similarly, for the left reservoir one obtains

$$I_L^u = \int_{-\infty}^{+\infty} \frac{dE}{h} E [\tau_{LR}(E) f_R(E) - \tau_{RL}(E) f_L(E)] + \frac{\Omega}{2\pi} \sum_{\beta=L,R} \int_{-\infty}^{+\infty} dE \langle n(E) \rangle_{L\beta} f_\beta(E). \quad (\text{B10})$$

Finally, substituting Eqs. (B9) and (B10) in Eq. (B1), the power injected by the applied voltage can be written as

$$P_{in} = \int_{-\infty}^{+\infty} \frac{dE}{h} E [\tau_{RL}(E) f_L(E) - \tau_{LR}(E) f_R(E)] + \tau_{LR}(E) f_R(E) - \tau_{RL}(E) f_L(E) + \frac{\Omega}{2\pi} \sum_{\beta=L,R} \int_{-\infty}^{+\infty} dE \langle n(E) \rangle_{R\beta} f_\beta(E) + \langle n(E) \rangle_{L\beta} f_\beta(E) = \frac{\Omega}{2\pi} \sum_{\alpha,\beta=L,R} \int_{-\infty}^{+\infty} dE \langle n(E) \rangle_{\alpha\beta} f_\beta(E), \quad (\text{B11})$$

with is the expression reported in Eq. (34) of the main text. The same result can be obtained in terms of heat and charge currents, indeed one has

$$P_{in} = I_L^u + I_R^u = -\Delta V I_R^e + I_L^h + I_R^h, \quad (\text{B12})$$

- ¹ S. Carnot, *Réflexions sur la puissance motrice du feu et sur les machines propres à développer cette puissance* (Bachelier, Paris, 1824).
- ² E. Fermi, *Thermodynamics* (Dover Publications, 1956).
- ³ M. Esposito, U. Harbola, and S. Mukamel, *Rev. Mod. Phys.* **81**, 1665 (2009), URL <https://link.aps.org/doi/10.1103/RevModPhys.81.1665>.
- ⁴ M. Campisi, P. Hänggi, and P. Talkner, *Rev. Mod. Phys.* **83**, 771 (2011), URL <https://link.aps.org/doi/10.1103/RevModPhys.83.771>.
- ⁵ R. Kosloff, *Entropy* **15**, 2100 (2013), ISSN 1099-4300, URL <https://www.mdpi.com/1099-4300/15/6/2100>.
- ⁶ D. Gelbwaser-Klimovsky, W. Niedenzu, and G. Kurizki (Academic Press, 2015), vol. 64 of *Advances In Atomic, Molecular, and Optical Physics*, pp. 329–407, URL <https://www.sciencedirect.com/science/article/pii/S1049250X15000130>.
- ⁷ B. Sothmann, R. Sánchez, and A. N. Jordan, *Nanotechnology* **26**, 032001 (2014), URL <https://dx.doi.org/10.1088/0957-4484/26/3/032001>.
- ⁸ M. Campisi and R. Fazio, *Journal of Physics A: Mathematical and Theoretical* **49**, 345002 (2016), URL <https://dx.doi.org/10.1088/1751-8113/49/34/345002>.
- ⁹ S. Vinjanampathy and J. Anders, *Contemporary Physics* **57**, 545 (2016), URL <https://doi.org/10.1080/00107514.2016.1201896>.
- ¹⁰ J. Gould, M. Huber, A. Riera, L. del Rio, and P. Skrzypczyk, *Journal of Physics A: Mathematical and Theoretical* **49**, 143001 (2016), URL <https://dx.doi.org/10.1088/1751-8113/49/14/143001>.
- ¹¹ G. Benenti, G. Casati, K. Saito, and R. S. Whitney, *Physics Reports* **694**, 1 (2017), ISSN 0370-1573, funda-

mental aspects of steady-state conversion of heat to work at the nanoscale, URL <https://www.sciencedirect.com/science/article/pii/S0370157317301540>.

- ¹² J. P. Pekola and B. Karimi, *Rev. Mod. Phys.* **93**, 041001 (2021), URL <https://link.aps.org/doi/10.1103/RevModPhys.93.041001>.
- ¹³ G. T. Landi and M. Paternostro, *Rev. Mod. Phys.* **93**, 035008 (2021), URL <https://link.aps.org/doi/10.1103/RevModPhys.93.035008>.
- ¹⁴ G. T. Landi, D. Poletti, and G. Schaller, *Rev. Mod. Phys.* **94**, 045006 (2022), URL <https://link.aps.org/doi/10.1103/RevModPhys.94.045006>.
- ¹⁵ P. P. Potts, *Quantum thermodynamics* (2024), 2406.19206, URL <https://arxiv.org/abs/2406.19206>.
- ¹⁶ S. Deffner and S. Campbell, *Quantum Thermodynamics*, 2053-2571 (Morgan and Claypool Publishers, 2019), ISBN 978-1-64327-658-8, URL <https://dx.doi.org/10.1088/2053-2571/ab21c6>.
- ¹⁷ S. Bhattacharjee and A. Dutta, *The European Physical Journal B* **94** (2021).
- ¹⁸ L. Arrachea, *Reports on Progress in Physics* **86**, 036501 (2023), URL <https://dx.doi.org/10.1088/1361-6633/acb06b>.
- ¹⁹ L. M. Cangemi, V. Cataudella, G. Benenti, M. Sasseti, and G. De Filippis, *Phys. Rev. B* **102**, 165418 (2020), URL <https://link.aps.org/doi/10.1103/PhysRevB.102.165418>.
- ²⁰ F. Cavaliere, L. Razzoli, M. Carrega, G. Benenti, and M. Sasseti, *iScience* **26**, 106235 (2023).
- ²¹ L. D. Hicks and M. S. Dresselhaus, *Phys. Rev. B* **47**, 12727 (1993), URL <https://link.aps.org/doi/10.1103/PhysRevB.47.12727>.

- ²² L. D. Hicks and M. S. Dresselhaus, Phys. Rev. B **47**, 16631 (1993), URL <https://link.aps.org/doi/10.1103/PhysRevB.47.16631>.
- ²³ L. D. Hicks, T. C. Harman, X. Sun, and M. S. Dresselhaus, Phys. Rev. B **53**, R10493 (1996), URL <https://link.aps.org/doi/10.1103/PhysRevB.53.R10493>.
- ²⁴ M. Terraneo, M. Peyrard, and G. Casati, Phys. Rev. Lett. **88**, 094302 (2002), URL <https://link.aps.org/doi/10.1103/PhysRevLett.88.094302>.
- ²⁵ N. Li, J. Ren, L. Wang, G. Zhang, P. Hänggi, and B. Li, Rev. Mod. Phys. **84**, 1045 (2012), URL <https://link.aps.org/doi/10.1103/RevModPhys.84.1045>.
- ²⁶ S. Ryu, R. López, L. Serra, and D. Sánchez, Nat. Commun. **13**, 2512 (2022), URL <https://doi.org/10.1038/s41467-022-30039-7>.
- ²⁷ G. Benenti, G. Casati, and J. Wang, Phys. Rev. Lett. **110**, 070604 (2013), URL <https://link.aps.org/doi/10.1103/PhysRevLett.110.070604>.
- ²⁸ E. Bocquillon, V. Freulon, F. D. Parmentier, J.-M. Berroir, B. Plaçais, C. Wahl, J. Rech, T. Jonckheere, T. Martin, C. Grenier, et al., Annalen der Physik **526**, 1 (2014), URL <https://onlinelibrary.wiley.com/doi/abs/10.1002/andp.201300181>.
- ²⁹ D. Ferraro and M. Sasseti, in *Encyclopedia of Condensed Matter Physics (Second Edition)*, edited by T. Chakraborty (Academic Press, Oxford, 2024), pp. 924–933, second edition ed., ISBN 978-0-323-91408-6, URL <https://www.sciencedirect.com/science/article/pii/B9780323908009000731>.
- ³⁰ X.-G. Wen, Adv. Phys. **44**, 405 (1995), URL <https://doi.org/10.1080/00018739500101566>.
- ³¹ J. von Delft and H. Schoeller, Annalen der Physik **510**, 225 (1998), URL <https://onlinelibrary.wiley.com/doi/abs/10.1002/andp.19985100401>.
- ³² L. S. Levitov, H. Lee, and G. B. Lesovik, Journal of Mathematical Physics **37**, 4845 (1996), URL <https://doi.org/10.1063/1.531672>.
- ³³ J. Dubois, T. Jullien, C. Grenier, P. Degiovanni, P. Roulleau, and D. C. Glattli, Phys. Rev. B **88**, 085301 (2013), URL <https://link.aps.org/doi/10.1103/PhysRevB.88.085301>.
- ³⁴ C. Grenier, J. Dubois, T. Jullien, P. Roulleau, D. C. Glattli, and P. Degiovanni, Phys. Rev. B **88**, 085302 (2013), URL <https://link.aps.org/doi/10.1103/PhysRevB.88.085302>.
- ³⁵ E. V. Sukhorukov and V. V. Cheianov, Phys. Rev. Lett. **99**, 156801 (2007), URL <https://link.aps.org/doi/10.1103/PhysRevLett.99.156801>.
- ³⁶ I. P. Levkivskiy and E. V. Sukhorukov, Phys. Rev. B **78**, 045322 (2008), URL <https://link.aps.org/doi/10.1103/PhysRevB.78.045322>.
- ³⁷ P. Degiovanni, C. Grenier, G. Fève, C. Altimiras, H. le Sueur, and F. Pierre, Phys. Rev. B **81**, 121302 (2010), URL <https://link.aps.org/doi/10.1103/PhysRevB.81.121302>.
- ³⁸ C. Wahl, J. Rech, T. Jonckheere, and T. Martin, Phys. Rev. Lett. **112**, 046802 (2014), URL <https://link.aps.org/doi/10.1103/PhysRevLett.112.046802>.
- ³⁹ D. Ferraro, B. Roussel, C. Cabart, E. Thibierge, G. Fève, C. Grenier, and P. Degiovanni, Phys. Rev. Lett. **113**, 166403 (2014), URL <https://link.aps.org/doi/10.1103/PhysRevLett.113.166403>.
- ⁴⁰ A. O. Slobodeniuk, E. G. Idrisov, and E. V. Sukhorukov, Phys. Rev. B **93**, 035421 (2016), URL <https://link.aps.org/doi/10.1103/PhysRevB.93.035421>.
- ⁴¹ G. Rebora, M. Acciai, D. Ferraro, and M. Sasseti, Phys. Rev. B **101**, 245310 (2020), URL <https://link.aps.org/doi/10.1103/PhysRevB.101.245310>.
- ⁴² E. G. Idrisov, I. P. Levkivskiy, E. V. Sukhorukov, and T. L. Schmidt, Phys. Rev. B **106**, 085405 (2022), URL <https://link.aps.org/doi/10.1103/PhysRevB.106.085405>.
- ⁴³ C. Altimiras, H. le Sueur, U. Gennser, A. Cavanna, D. Mailly, and F. Pierre, Nature Physics **6**, 34 (2010), URL <https://doi.org/10.1038/nphys1429>.
- ⁴⁴ E. Bocquillon, V. Freulon, J.-M. Berroir, P. Degiovanni, B. Plaçais, A. Cavanna, Y. Jin, and G. Fève, Nat. Commun. **4**, 1839 (2013), URL <https://doi.org/10.1038/ncomms2788>.
- ⁴⁵ R. H. Rodriguez, F. D. Parmentier, D. Ferraro, P. Roulleau, U. Gennser, A. Cavanna, M. Sasseti, F. Portier, D. Mailly, and P. Roche, Nat. Commun. **11**, 2426 (2020), URL <https://doi.org/10.1038/s41467-020-16331-4>.
- ⁴⁶ E. Frigerio, G. Rebora, M. Ruelle, H. Souquet-Basiège, Y. Jin, U. Gennser, A. Cavanna, B. Plaçais, E. Baudin, J. M. Berroir, et al., *Gate tunable edge magnetoplasmon resonators* (2024), 2404.18204, URL <https://arxiv.org/abs/2404.18204>.
- ⁴⁷ E. V. Sukhorukov, Physica E: Low-dimensional Systems and Nanostructures **77**, 191 (2016), ISSN 1386-9477, URL <https://www.sciencedirect.com/science/article/pii/S1386947715302836>.
- ⁴⁸ A. Crépieux, P. Devillard, and T. Martin, Phys. Rev. B **69**, 205302 (2004), URL <https://link.aps.org/doi/10.1103/PhysRevB.69.205302>.
- ⁴⁹ D. L. Kovrizhin and J. T. Chalker, Phys. Rev. Lett. **109**, 106403 (2012), URL <https://link.aps.org/doi/10.1103/PhysRevLett.109.106403>.
- ⁵⁰ A. Braggio, D. Ferraro, M. Carrega, N. Magnoli, and M. Sasseti, New Journal of Physics **14**, 093032 (2012), URL <https://dx.doi.org/10.1088/1367-2630/14/9/093032>.
- ⁵¹ J. Rech, D. Ferraro, T. Jonckheere, L. Vannucci, M. Sasseti, and T. Martin, Phys. Rev. Lett. **118**, 076801 (2017), URL <https://link.aps.org/doi/10.1103/PhysRevLett.118.076801>.
- ⁵² L. Vannucci, F. Ronetti, J. Rech, D. Ferraro, T. Jonckheere, T. Martin, and M. Sasseti, Phys. Rev. B **95**, 245415 (2017), URL <https://link.aps.org/doi/10.1103/PhysRevB.95.245415>.
- ⁵³ I. Safi, The European Physical Journal B **12**, 451 (1999), URL <https://doi.org/10.1007/s100510051026>.
- ⁵⁴ R. A. Jalabert, A. D. Stone, and Y. Alhassid, Phys. Rev. Lett. **68**, 3468 (1992), URL <https://link.aps.org/doi/10.1103/PhysRevLett.68.3468>.
- ⁵⁵ Y. Alhassid, Rev. Mod. Phys. **72**, 895 (2000), URL <https://link.aps.org/doi/10.1103/RevModPhys.72.895>.
- ⁵⁶ M. Moskalets and M. Büttiker, Phys. Rev. B **78**, 035301 (2008), URL <https://link.aps.org/doi/10.1103/PhysRevB.78.035301>.
- ⁵⁷ M. Moskalets, Phys. Rev. Lett. **112**, 206801 (2014), URL <https://link.aps.org/doi/10.1103/PhysRevLett.112.206801>.
- ⁵⁸ M. V. Moskalets, *Scattering Matrix Approach to Non-Stationary Quantum Transport* (IMPERIAL COLLEGE PRESS, 2011), URL <https://www.worldscientific.com/doi/abs/10.1142/p822>.
- ⁵⁹ F. Battista, F. Haupt, and J. Splettstoesser, Phys. Rev. B **90**, 085418 (2014), URL <https://link.aps.org/doi/10.1103/PhysRevB.90.085418>.

- 1103/PhysRevB.90.085418.
- ⁶⁰ Y. Blanter and M. Büttiker, *Physics Reports* **336**, 1 (2000), ISSN 0370-1573, URL <https://www.sciencedirect.com/science/article/pii/S0370157399001234>.
- ⁶¹ Y. Dubi, Y. Meir, and Y. Avishai, *Phys. Rev. B* **74**, 205314 (2006), URL <https://link.aps.org/doi/10.1103/PhysRevB.74.205314>.
- ⁶² D. A. Ivanov, H. W. Lee, and L. S. Levitov, *Phys. Rev. B* **56**, 6839 (1997), URL <https://link.aps.org/doi/10.1103/PhysRevB.56.6839>.
- ⁶³ J. Keeling, I. Klich, and L. S. Levitov, *Phys. Rev. Lett.* **97**, 116403 (2006), URL <https://link.aps.org/doi/10.1103/PhysRevLett.97.116403>.
- ⁶⁴ J. Dubois, T. Jullien, F. Portier, P. Roche, A. Cavanna, Y. Jin, W. Wegscheider, P. Roulleau, and D. C. Glattli, *Nature* **502**, 659 (2013), URL <https://doi.org/10.1038/nature12713>.
- ⁶⁵ D. Glattli and P. Roulleau, *Phys. E* **76**, 216 (2016), ISSN 1386-9477, URL <https://www.sciencedirect.com/science/article/pii/S1386947715302617>.
- ⁶⁶ C. Bäuerle, D. C. Glattli, T. Meunier, F. Portier, P. Roche, P. Roulleau, S. Takada, and X. Waintal, *Rep. Prog. Phys.* **81**, 056503 (2018), URL <https://dx.doi.org/10.1088/1361-6633/aaa98a>.
- ⁶⁷ M. Aluffi, T. Vasselon, S. Ouacel, H. Edlbauer, C. Geffroy, P. Roulleau, D. C. Glattli, G. Georgiou, and C. Bäuerle, *Phys. Rev. Appl.* **20**, 034005 (2023), URL <https://link.aps.org/doi/10.1103/PhysRevApplied.20.034005>.
- ⁶⁸ D. C. Glattli and P. S. Roulleau, *physica status solidi (b)* **254**, 1600650 (2017), URL <https://onlinelibrary.wiley.com/doi/abs/10.1002/pssb.201600650>.
- ⁶⁹ D. Ferraro, F. Ronetti, J. Rech, T. Jonckheere, M. Sasseti, and T. Martin, *Phys. Rev. B* **97**, 155135 (2018), URL <https://link.aps.org/doi/10.1103/PhysRevB.97.155135>.
- ⁷⁰ J. C. Y. Teo and C. L. Kane, *Phys. Rev. B* **79**, 235321 (2009), URL <https://link.aps.org/doi/10.1103/PhysRevB.79.235321>.
- ⁷¹ A. Ström and H. Johannesson, *Phys. Rev. Lett.* **102**, 096806 (2009), URL <https://link.aps.org/doi/10.1103/PhysRevLett.102.096806>.
- ⁷² D. Ferraro, G. Dolcetto, R. Citro, F. Romeo, and M. Sasseti, *Phys. Rev. B* **87**, 245419 (2013), URL <https://link.aps.org/doi/10.1103/PhysRevB.87.245419>.
- ⁷³ C. L. Kane and M. P. A. Fisher, *Phys. Rev. B* **51**, 13449 (1995), URL <https://link.aps.org/doi/10.1103/PhysRevB.51.13449>.
- ⁷⁴ S.-S. Lee, S. Ryu, C. Nayak, and M. P. A. Fisher, *Phys. Rev. Lett.* **99**, 236807 (2007), URL <https://link.aps.org/doi/10.1103/PhysRevLett.99.236807>.
- ⁷⁵ M. Carrega, D. Ferraro, A. Braggio, N. Magnoli, and M. Sasseti, *New Journal of Physics* **14**, 023017 (2012), URL <https://dx.doi.org/10.1088/1367-2630/14/2/023017>.
- ⁷⁶ M. F. Ludovico, M. Moskalets, D. Sánchez, and L. Arachea, *Phys. Rev. B* **94**, 035436 (2016), URL <https://link.aps.org/doi/10.1103/PhysRevB.94.035436>.
- ⁷⁷ S. Traverso, M. Sasseti, and N. Traverso Ziani, *npj Quantum Material* **9**, 1 (2024).